https://doi.org/10.5194/egusphere-2026-4540
Preprint. Discussion started: 30 July 2026

Forecasting different types of avalanches based on snowpack and snowfall/snowmelt conditions on the Southeastern Tibetan Plateau

Xiaoqian Fu[1,2,4], Jiansheng Hao[1,2,4,*], Peng Cui[1,2,3], Yan Wang[1,2,4], Guoqing Chen[1,2,4]

[1]Key Laboratory of Mountain Hazards and Engineering Resilience, Institute of Geographic Sciences and Natural Resources Research, Chinese Academy of Sciences, Beijing 100101, China;
[2]College of Resources and Environment, University of Chinese Academy of Sciences, Beijing 100049, China;
[3]China-Pakistan Joint Research Center on Earth Sciences, Islamabad 45320, Pakistan;
[4]Joint Laboratory of Mountain Hazard Prevention and Mitigation, Institute of Geographic Sciences and Natural Resources Research, Chinese Academy of Sciences (CAS), Beijing 100101, China;

Correspondence to: Jiansheng Hao (haojs@igsnrr.ac.cn)

Abstract. Reliable avalanche forecasting is essential for protecting mountain communities and transportation corridors, but estimating avalanche occurrence from monitored meteorological and snowpack conditions remains difficult. Operational assessments often rely primarily on meteorological thresholds, although avalanche responses depend on both type-specific triggering process and the snowpack conditions. Using meteorological, pre-event snowpack, and avalanche observations collected during the 2024 and 2025 snow seasons, we analysed 37 recorded avalanche events, together with corresponding non-avalanche periods. Separate logistic-regression models were developed for dry- and wet-snow avalanches using the intensity and duration of the preceding snowfall or snowmelt process and background snow depth. Their performance was compared with otherwise identical models excluding snow depth. Under leave-one-out cross-validation, including background snow depth increased the area under the receiver operating characteristic curve from 0.72 to 0.83 for dry-snow avalanches and from 0.85 to 0.94 for wet-snow avalanches. For wet-snow avalanches, the true-positive rate increased from 0.79 to 0.92, while the false-positive rate decreased from 0.21 to 0.12. These results demonstrate that pre-event snowpack conditions provides predictive information beyond meteorological forcing alone and improves avalanche forecasting, particularly for wet-snow avalanches.

1 Introduction

Climate warming is altering snowfall regimes, snowmelt timing, and rain–snow transitions in mountain regions, thereby reshaping the environmental conditions associated with cryospheric hazards (Li et al., 2024). In high mountains, snow avalanches are among the most consequential gravity-driven natural hazards. Owing to their sudden release, rapid movement, and potentially long runout distances, avalanches pose persistent threats to mountain communities, transportation corridors, and critical infrastructure (Acharya et al., 2023). At the same time, the expansion of hydropower facilities and high-elevation transportation networks is increasing the exposure of people and infrastructure to avalanche hazards. This growing interaction

https://doi.org/10.5194/egusphere-2026-4540
Preprint. Discussion started: 30 July 2026

between avalanche occurrence and socioeconomic exposure highlights the need for reliable monitoring and forecasting systems in mountain regions.

Avalanche forecasting requires a quantitative characterization of how meteorological forcing interacts with the pre-event snowpack conditions to influence the probability of avalanche release. However, the dominant triggering processes and failure mechanisms vary among avalanche types. Dry-snow avalanches, which predominantly occur under sub-freezing conditions, are often associated with rapid new-snow accumulation and the resulting increase in load on the pre-event snowpack (McClung, 2009; Schweizer et al., 2003b). For dry-snow slab avalanches, this additional loading can promote failure in a weak layer and subsequent crack propagation through the snowpack, eventually resulting in slab release. Consequently, cumulative new snow and snowfall intensity are commonly used as key indicators in the assessment and forecasting of dry-snow avalanche hazard (Wei et al., 2025). Empirical studies in the Swiss Alps have reported a substantial increase in avalanche probability when 1–3 d cumulative new-snow amounts reach approximately 30–50 cm (Schweizer et al., 2003a). Beyond fixed empirical thresholds, recent studies have increasingly evaluated the balance between meteorological loading and snowpack stability to improve probabilistic predictions of natural dry-snow avalanche activity (Mayer et al., 2023).

In contrast, wet-snow avalanches typically occur during periods of sustained warming, rain-on-snow events, or active snowmelt. As air temperature rises and liquid water enters the snowpack, water infiltration alters grain-scale bonding, enhances snow deformation, and may lead to water accumulation along stratigraphic interfaces. Together, these processes reduce snowpack strength and promote wet-snow instability and avalanche release (Hendrick et al., 2023; Mayer et al., 2024). Consequently, air-temperature evolution, surface energy input, and liquid-water availability are commonly used as predictors of wet-snow avalanche activity (Bellaire et al., 2017). A two-decade observational record from the Dischma Valley, Switzerland, showed that natural wet-snow avalanche activity was frequently preceded by 3–5 consecutive days with mean daily air temperatures above 0 °C (Baggi and Schweizer, 2009). From an energy-balance perspective, observations in the Davos region indicated that a cumulative positive net energy input of approximately 1.2 MJ m^{-2} over 3 d was associated with periods of widespread wet-snow avalanche activity (Mitterer and Schweizer, 2013). Furthermore, analyses of long-term observational records in North America showed that, during sustained spring warming, liquid-water percolation and its accumulation above persistent weak layers may contribute to the release of large wet-snow avalanches (Marienthal et al., 2015). Nevertheless, although these meteorological indicators capture important aspects of wet-snow avalanche formation, their predictive performance may vary substantially among locations and snowpack conditions, resulting in false alarms and missed events when fixed thresholds are applied (Morin et al., 2020).

This limitation arises because avalanche release depends not only on meteorological forcing but also on snowpack conditions, which vary substantially across space and time (Monti et al., 2016; Schweizer et al., 2003a). Consequently, similar snowfall or melt forcing can produce contrasting stability responses under different snowpack conditions. Fixed meteorological thresholds may therefore fail to capture this state dependence, resulting in false alarms or missed events. Recent studies have shown that combining meteorological observations with snowpack process simulations can improve avalanche prediction

https://doi.org/10.5194/egusphere-2026-4540
Preprint. Discussion started: 30 July 2026

relative to meteorology-only approaches (Pérez-Guillén et al., 2022). These findings highlight the value of incorporating indicators of the snowpack condition into avalanche forecasting models.

Focusing on an avalanche-prone high mountain valley in the southeastern Tibetan Plateau, this study compiles an event database using a dedicated in situ monitoring network that integrates meteorological, snowpack, and avalanche observations. Background snow depth is used as an observable indicator of pre-event snowpack conditions. Separate logistic regression models are developed for dry- and wet-snow avalanches to quantify the combined contributions of forcing intensity, forcing duration, and background snow depth to avalanche occurrence probability. These models are compared with meteorology-only baselines to assess whether the inclusion of background snow depth improves event discrimination and reduces false-alarm rates. By extending fixed meteorological thresholds to a probabilistic framework that accounts for antecedent snow accumulation, this study provides an interpretable quantitative basis for regional avalanche monitoring and forecasting.

2. Study area and data

2.1 Study area

Galongla Valley is located on the southeastern margin of the Tibetan Plateau, China, within the lower Yarlung Zangbo River basin (Fig. 1a). The region lies along a major monsoonal moisture-transport pathway, through which moisture from the Bay of Bengal is transported northward via the Yarlung Zangbo Grand Canyon, contributing substantially to precipitation along the canyon corridor (Yuan et al., 2023). Elevation within the study area ranges from 2723 to 5699 m. The terrain is steep and deeply dissected, with a mean slope angle of approximately 34.0° and maximum values exceeding 70°. Numerous confined gullies connect high-elevation snow accumulation areas with the valley floor and adjacent transportation corridor, providing favourable topographic conditions for avalanche release and channelised downslope movement. The main snow season generally extends from late December to June, and the local snow regime exhibits pronounced characteristics of a maritime snow climate (Wen et al., 2024). Frequent snowfall, episodic warming, and recurrent melt–freeze conditions produce substantial temporal changes in snowpack properties, creating favourable conditions for both snowfall-induced dry-snow avalanches and snowmelt-induced wet-snow avalanches. Galongla Valley was therefore selected as a representative site for integrated observations of meteorological, snowpack, and avalanche activity. Field investigations identified 23 avalanche paths, 12 of which directly threaten local transportation routes (Fig. 1b). To systematically monitor avalanche activity and its environmental controls, an integrated network of ten monitoring stations was deployed near the release zones of the avalanche paths posing the greatest threat to infrastructure (Fig. 1b, 1c).

https://doi.org/10.5194/egusphere-2026-4540
Preprint. Discussion started: 30 July 2026

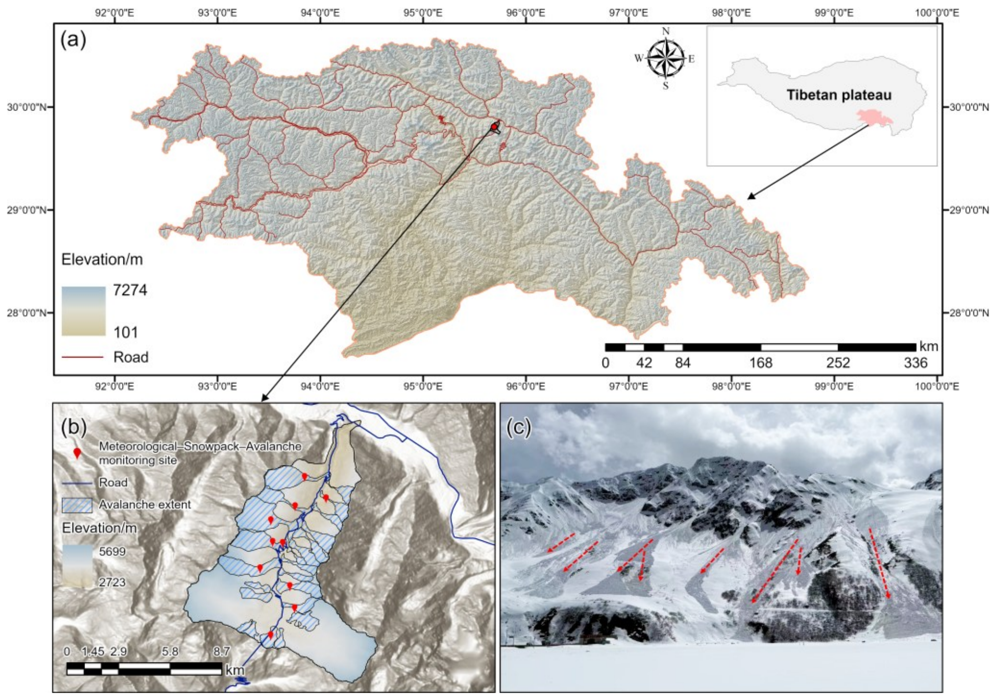

Figure 1. Overview of the study area and monitoring network. (a) Regional topography of the southeastern Tibetan Plateau, China, showing the location of the Galongla Valley. (b) Distribution of monitoring stations and mapped avalanche extents within the Galongla Valley. (c) Field photograph of Galongla Mountain showing avalanche paths.

2.2 Data

The meteorological and snowpack data used in this study were obtained from an integrated meteorological–snowpack–avalanche monitoring network that has been operating in the Galongla valley since 2023 (Fig. 2a). The stations are strategically located near the potential release zones of major avalanche-prone slopes at elevations of 3600–3700 m, enabling the effective capture of key meteorological forcing and snowpack evolution processes within avalanche source areas. Each station consists of an automatic weather station, a weighing precipitation gauge, a snow stake, and a thermal infrared camera (Fig. 2b), with meteorological and snow-depth variables recorded at a temporal resolution of 1 min. During the snow season, avalanche events affecting transportation corridors and adjacent slopes are documented in real time using integrated video surveillance systems, allowing for the systematic collection of essential event information, including occurrence time and avalanche type.

https://doi.org/10.5194/egusphere-2026-4540
Preprint. Discussion started: 30 July 2026

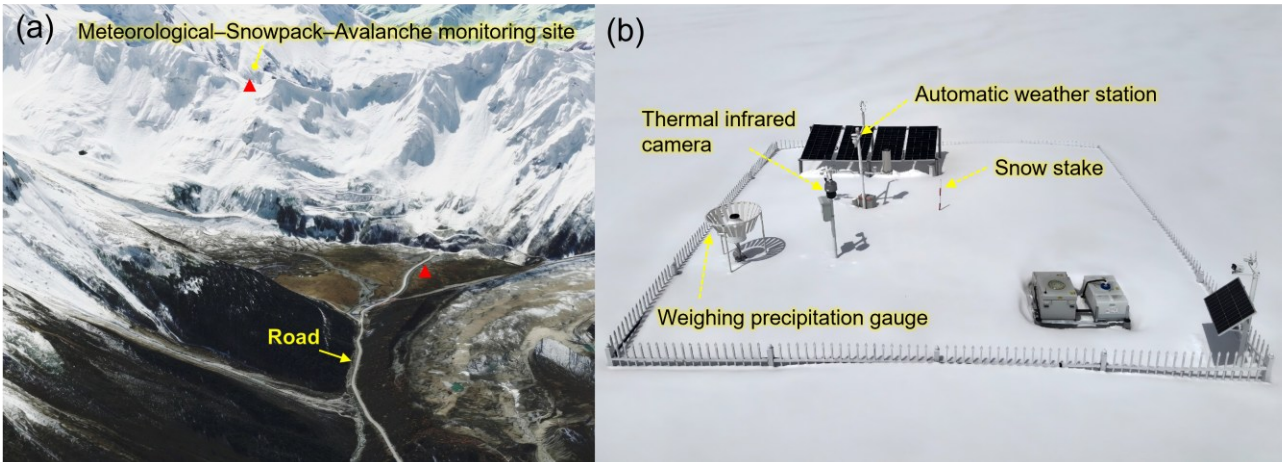

Figure 2: Integrated meteorological–snowpack–avalanche monitoring system in Galongla Valley. (a) Locations of representative monitoring stations; (b) Field configuration of the monitoring network.

2.3 Predictor variables

Dry-snow avalanches predominantly occur under subfreezing conditions, typically following intense snowfall during sustained cold periods. The primary triggering mechanism is rapid mechanical loading caused by the accumulation of new snow. Under these conditions, snow grains are generally dry and unconsolidated, with weak intergranular bonding. Upon release, dry-snow avalanches can reach velocities of several tens of metres per second and propagate as powder-snow clouds or highly fragmented dense flows along steep avalanche paths (Fig. 3a), before depositing in runout zones where they may block transportation corridors (Fig. 3b). Consequently, snowfall is recognized as the principal driver of dry-snow avalanche initiation. To quantitatively characterise this dynamic loading process, we define a snowfall event as a continuous period with measurable snowfall and a concurrent increase in snow depth. For avalanche samples, the triggering process was defined as the last snowfall event preceding the recorded avalanche occurrence time (t_{event}), and any ongoing event was truncated at t_{event}. Snowfall Duration (SFD) was calculated as the duration of this event segment, and Snowfall Intensity (SFI) as the corresponding cumulative snowfall divided by SFD, representing the mean rate of snow loading. In parallel, the snow depth recorded at the onset of the event is defined as Background Snow Depth (SD), which serves as a quantitative proxy for the pre-event snowpack conditions.

https://doi.org/10.5194/egusphere-2026-4540
Preprint. Discussion started: 30 July 2026

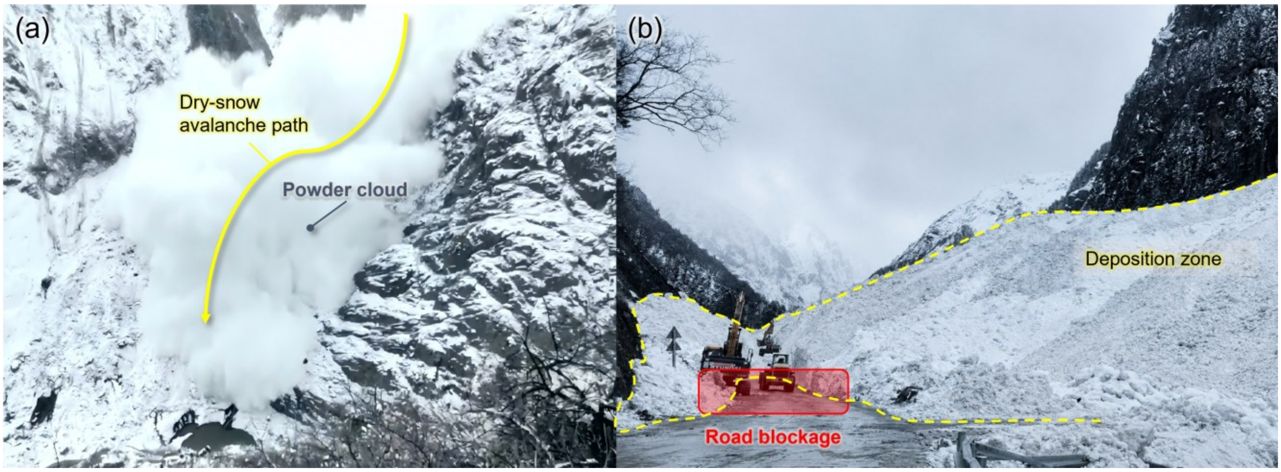

Figure 3: Typical movement and deposition characteristics of dry-snow avalanches. (a) Dry-snow avalanche path with a powder cloud; (b) Avalanche deposition causing road blockage.

Wet-snow avalanches predominantly occur during warming periods or rain-on-snow conditions, and are primarily triggered by rapid air-temperature increases or liquid-water input. The percolation of meltwater promotes snowpack structural weakening and reduces shear strength, thereby increasing the susceptibility of the slab to overall instability. Although wet-snow avalanches generally propagate at lower velocities than dry-snow avalanches, they often involve substantial mass and can exert persistent and destructive impact pressures. These events typically develop as dense, water-rich flows with a high capacity to entrain debris and ice fragments as they move downslope along confined avalanche paths (Fig. 4a). Owing to their high bulk density and large mass, wet-snow avalanches commonly form compact depositional masses in runout zones, which can severely obstruct roads and transportation corridors (Fig. 4b). Consequently, snowmelt is identified as a key driver of wet-snow avalanche initiation. In this study, we define a snowmelt event as a distinct period during which air temperature exceeds 0 °C and snow depth continuously decreases. For avalanche samples, the triggering process was defined as the last snowmelt event preceding t_{event}, and any ongoing event was truncated at the avalanche occurrence time. Snowmelt Duration (SMD) was calculated as the duration of this event segment, whereas Snowmelt Intensity (SMI) was calculated as the corresponding cumulative snow-depth loss divided by SMD. Similarly, the snow depth recorded at the onset of the event is defined as Background Snow Depth (SD), serving as a quantitative indicator of the pre-event snowpack conditions before meltwater forcing.

https://doi.org/10.5194/egusphere-2026-4540
Preprint. Discussion started: 30 July 2026

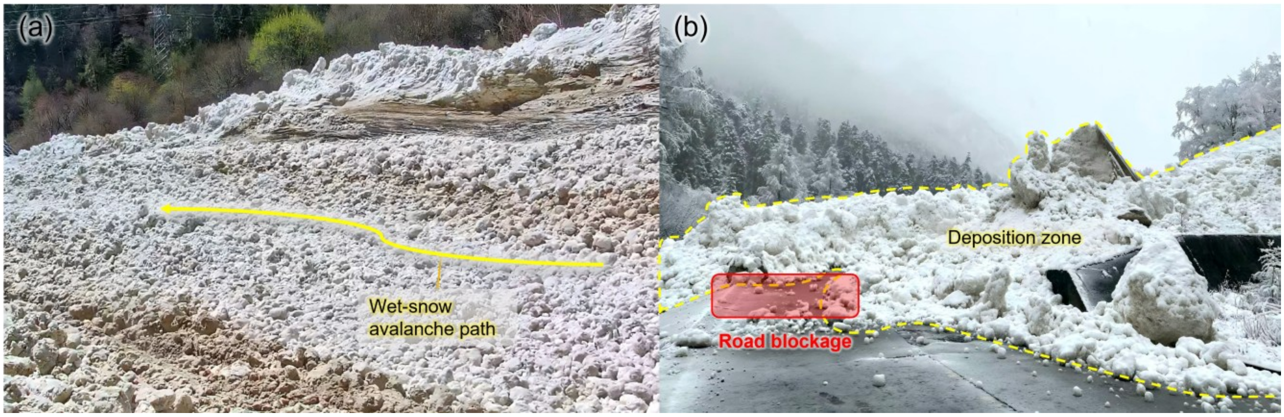

Figure 4: Typical movement and deposition characteristics of wet-snow avalanches. (a) Wet-snow avalanche path; (b) Avalanche deposition causing road blockage.

2.4 Construction of positive and negative samples

For each recorded dry- or wet-snow avalanche, candidate meteorological processes were identified within a 3-d retrospective window at the corresponding monitoring station using the same process-identification criteria described above. The most recent snowfall or snowmelt event block preceding the recorded avalanche time was treated as the positive sample, with all variables calculated only up to the avalanche occurrence time. Earlier event blocks within the same retrospective window were considered candidate negative samples. To avoid including processes associated with the same triggering episode, the positive event block and all adjacent blocks within a 12 h buffer were excluded. Candidate blocks overlapping any known avalanche occurrence at the same station and of the same avalanche type were also removed using the full avalanche-time inventory. A maximum of three negative samples was retained for each positive sample, prioritising temporally closer but clearly separated events. The predictor variables for positive and negative samples were calculated using identical definitions to ensure direct comparability. After screening, the dry-snow dataset comprised 13 positive and 39 negative samples, and the wet-snow dataset comprised 24 positive and 72 negative samples.

2.5 Statistical modelling and performance evaluation

Within a statistical modelling framework, this study employs logistic regression (LR) to develop an avalanche forecasting model that integrates snowpack conditions with meteorological thresholds, hereafter referred to as the Snowpack–Meteorology Logistic Model (SMLM). The model uses meteorological and snowpack predictors, with avalanche occurrence or non-occurrence treated as the binary response variable (Fu et al.,2026). To reduce the influence of differences in physical magnitude and skewed variable distributions on parameter estimation, all input variables are subjected to a uniform logarithmic transformation before model fitting. The transformation is expressed as follows:

$$x_i' = \ln(1 + x_i) \,, \tag{1}$$

https://doi.org/10.5194/egusphere-2026-4540
Preprint. Discussion started: 30 July 2026

where x_i denotes the original input variable and x_i' denotes the transformed model input. In the space of log-transformed variables, the LR model is expressed as:

$$\mathrm{P}(\mathrm{Y}=1 \mid \mathrm{x})=\frac{1}{1+\exp\left[-\left(\mathrm{b}+\sum_{\mathrm{i}=1}^{\mathrm{k}} \mathrm{w}_{\mathrm{i}} \mathrm{x}_{\mathrm{i}}'\right)\right]}, \tag{2}$$

where $\mathrm{P}(\mathrm{Y}=1 \mid \mathrm{x})$ represents the conditional probability of avalanche occurrence, w_i is the regression coefficient for the *i-th* input variable, b is the intercept term, and k is the number of input variables. Model parameters are estimated using maximum likelihood estimation.

To ensure the robustness and reliability of the parameter estimates, multicollinearity among the predictors was assessed using the variance inflation factor (VIF). All VIF values were below the threshold of 3, indicating no substantial multicollinearity among the predictors (Zuur et al., 2010). In addition, to quantify uncertainty in the model parameters, a non-parametric bootstrap procedure was applied. Specifically, 1000 bootstrap resamples were generated with replacement, and the regression coefficients were repeatedly estimated to derive their corresponding 95% confidence intervals (CIs). A predictor was considered statistically significant at the 95% confidence level when its bootstrap-derived confidence interval did not include zero (Efron and Tibshirani, 1986).

The discriminative performance of the model was evaluated using leave-one-out cross-validation (LOOCV). In the LOOCV framework, one observation is withheld as the test sample in each iteration, whereas the remaining observations are used for model training. This procedure is repeated until out-of-fold predicted probabilities and their corresponding ground-truth labels are obtained for all observations (Hastie et al., 2009). Based on these predictions, we constructed a receiver operating characteristic (ROC) curve and calculated the area under the ROC curve (AUC) to quantify the overall discriminative ability of the model. The optimal probability threshold was determined by maximizing the Youden Index ($J = TPR - FPR$), where TPR and FPR denote the true positive rate and false positive rate (Youden, 1950). The predicted probabilities were then converted into binary classifications using this optimal threshold, and a confusion matrix was constructed (Table 1). Based on this matrix, a comprehensive set of performance metrics was calculated to evaluate classification performance, including TPR, FPR, true negative rate (TNR), false negative rate (FNR), precision, and F1-score (Fawcett, 2006). The mathematical formulations for these metrics are detailed in Eqs. (3) – (8).

Table 1. The Contingency Matrix

	Observed	
Predicted	Yes	No
Yes	TP	FP
No	FN	TN

$$\mathrm{TPR}=\frac{\mathrm{TP}}{\mathrm{TP}+\mathrm{FN}}, \tag{3}$$

$$\mathrm{FPR}=\frac{\mathrm{FP}}{\mathrm{FP}+\mathrm{TN}}, \tag{4}$$

$$\mathrm{TNR}=\frac{\mathrm{TN}}{\mathrm{TN}+\mathrm{FP}}, \tag{5}$$

https://doi.org/10.5194/egusphere-2026-4540
Preprint. Discussion started: 30 July 2026

$$\mathrm{FNR} = \frac{\mathrm{FN}}{\mathrm{TP+FN}}, \tag{6}$$

$$\mathrm{Precision} = \frac{\mathrm{TP}}{\mathrm{TP+FP}}, \tag{7}$$

$$\mathrm{F1} = \frac{2\mathrm{TP}}{2\mathrm{TP+FP+FN}}, \tag{8}$$

To quantitatively evaluate the incremental improvement in discriminative performance and model stability achieved by integrating snowpack conditions with meteorological thresholds, we constructed a baseline model driven exclusively by meteorological variables, hereafter referred to as the Meteorology-Only Logistic Model (MOLM). To ensure rigorous comparability, the integrated and baseline models were implemented using consistent definitions, model-construction procedures, and validation strategies. Specifically, the MOLM included only meteorological predictors: SFI and SFD for dry-snow avalanches and SMI and SMD for wet-snow avalanches. The SMLM additionally included background snow depth as a proxy for pre-event snowpack conditions.

3. Results

3.1 Avalanche activity characteristics

Based on monitoring data from two consecutive snow seasons (1 January–15 May in 2024 and 2025), we analysed mean snow depth and air temperature averaged across all monitoring stations in Galongla Valley (Fig. 5). During the 2024 snow season, the mean snow depth and mean air temperature were 0.17 m and -0.27 °C, respectively. In 2025, the corresponding values increased to 0.24 m and 1.16 °C. Overall, the main period of snow accumulation extended from January to March, with snow depth reaching seasonally high levels between late January and March. Thereafter, rising air temperatures were accompanied by rapid snow depletion, and the seasonal snow cover largely disappeared between April and May.

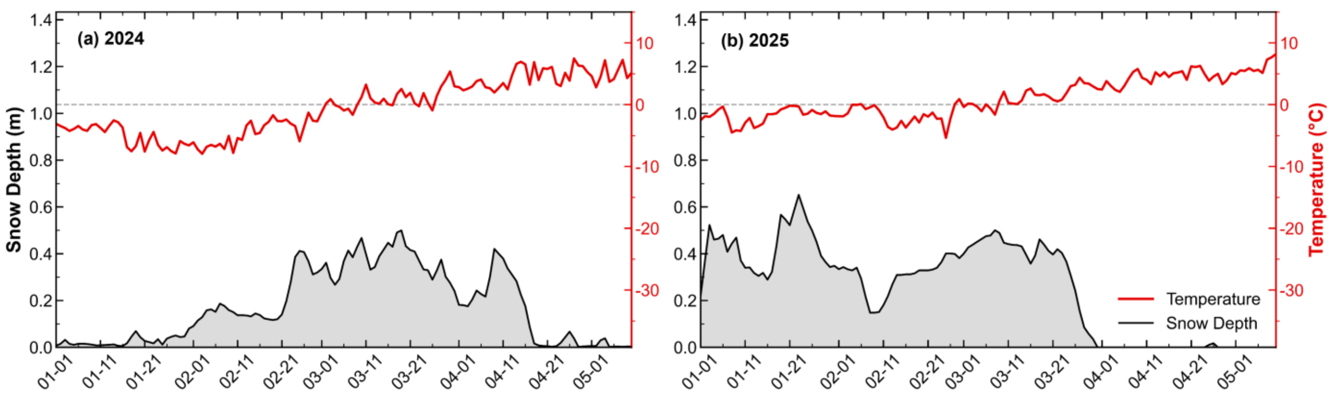

Figure 5: Time series of daily air temperature and snow depth in the Galongla valley during the 2024 and 2025 snow seasons. The red lines represent air temperature (°C), and the gray shaded areas indicate snow depth (m).

Consistent with the observed snowpack evolution, avalanche activity showed a concentrated seasonal distribution. During the 2024 and 2025 snow seasons, the monitoring network documented 37 avalanche events in total. Overall, avalanche activity

https://doi.org/10.5194/egusphere-2026-4540
Preprint. Discussion started: 30 July 2026

was concentrated from late February to mid-April, peaked during the first half of March, declined during the second half of March, and was not recorded after mid-April (Fig. 6). The two avalanche types differed primarily in the duration of their seasonal occurrence. Dry-snow avalanches (n = 13) occurred from late February to the end of March, with the highest frequency during the first half of March. Their temporal distribution coincided with the snowfall period and associated snowpack loading. Wet-snow avalanches (n = 24) occurred from late February to mid-April and likewise peaked during the first half of March. Their continuation into April coincided with rising air temperatures and snowpack depletion, conditions conducive to snowmelt and liquid-water infiltration.

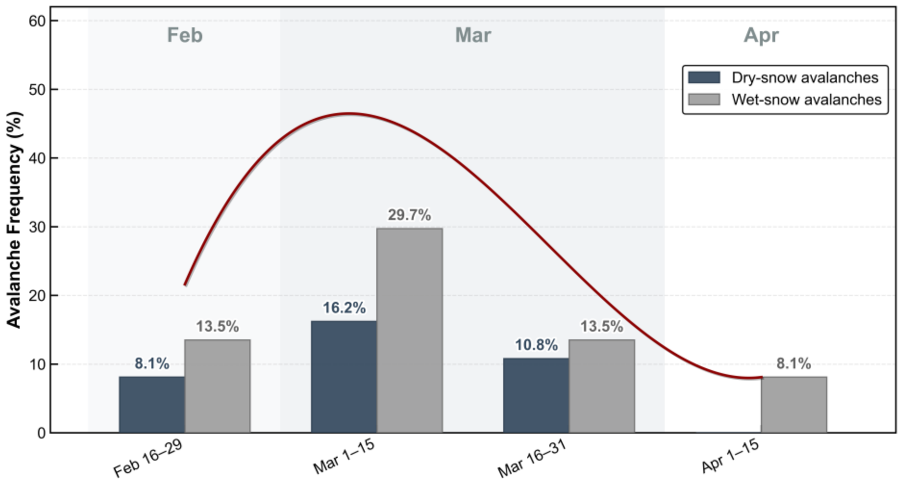

Figure 6: Seasonal distribution of avalanches

3.2 Model formulation and probabilistic relationships

3.2.1 Dry-snow avalanches

To establish a comparative baseline, we first constructed the dry-snow avalanche MOLM:

$$\ln\left(\frac{P}{1-P}\right) = -0.62 + 0.93\ln(1+\mathrm{SFI}) - 0.56\ln(1+\mathrm{SFD})\,, \tag{9}$$

In this baseline model, the regression coefficient for SFI is positive and statistically significant (95% CI [0.38, 1.52]), whereas the coefficient for SFD is negative but not statistically significant (95% CI [−1.36, 0.12]). A critical limitation of this model is that it defines a fixed decision boundary in the SFI–SFD phase space and is therefore independent of pre-event snowpack conditions. Consequently, it fails to distinguish the different avalanche probabilities associated with high- and low-SD conditions. To address this limitation, we incorporated SD as a fundamental state variable to construct the SMLM, formulated as follows:

$$\ln\left(\frac{P}{1-P}\right) = -0.78 + 0.55\ln(1+\mathrm{SFI}) - 0.62\ln(1+\mathrm{SFD}) + 1.93\ln(1+\mathrm{SD})\,, \tag{10}$$

In the dry-snow avalanche SMLM, the regression coefficient for SD is positive and exhibits the largest magnitude ($w_3 = 1.93$; 95% CI $[1.07, 2.71]$). Its confidence interval lies entirely above zero, indicating that greater background snow depth is

https://doi.org/10.5194/egusphere-2026-4540
Preprint. Discussion started: 30 July 2026

associated with a higher probability of dry-snow avalanche occurrence when the other variables are held constant. The coefficient for SFI remains positive ($w_1 = 0.55$), but its bootstrap-derived 95% CI $[-0.04, 1.21]$ slightly overlaps zero. This indicates a positive but statistically uncertain effect after background snow depth is incorporated into the model. Notably, the regression coefficient for SFD is negative and becomes statistically significant after SD is incorporated into the model ($w_2 = -0.62$; 95% CI $[-1.36, -0.02]$). This result indicates that, after accounting for background snow depth, longer snowfall duration is associated with a reduced probability of dry-snow avalanche occurrence.

The modelling results (Fig. 7a) delineate the critical threshold surface for dry-snow avalanches within the three-dimensional parameter space of SFI, SFD, and SD. The optimal probability threshold, determined by maximizing the Youden Index, is 0.41. This critical surface represents the joint effects of the three predictors on dry-snow avalanche probability. An examination of the two-dimensional cross-sectional projections reveals that the individual variables exert distinct influences on the snowpack system. Within the SFI–SD plane (Fig. 7b), a pronounced compensatory relationship between SFI and SD is evident. As SD increases, the critical SFI required to trigger an avalanche decreases substantially. Under conditions of a deep basal snowpack (high SD), even a marginal increment in SFI can drive the system across the critical boundary into the avalanche regime (red zone). In the SFI–SFD plane (Fig. 7c), SFI dominates the classification outcome. When SFI is exceptionally high (> 10 mm/h), samples predominantly fall into the avalanche regime, rendering the influence of SFD variations largely negligible. However, at low-to-moderate SFI levels, the critical threshold line exhibits a positive slope with increasing SFD. This indicates that within this specific range, SFD functions primarily as a regulatory variable rather than a direct triggering mechanism. Finally, in the SFD–SD plane (Fig. 7d), the system directly transitions into a high-risk state when SD is sufficiently deep (SD > 0.8 m), and this critical depth threshold does not diminish with prolonged SFD. Conversely, the critical boundary shifts slightly upward as SFD increases. This demonstrates that SFD mainly adjusts the position of the threshold boundary, contributing less directly to avalanche initiation than SD and SFI.

https://doi.org/10.5194/egusphere-2026-4540
Preprint. Discussion started: 30 July 2026

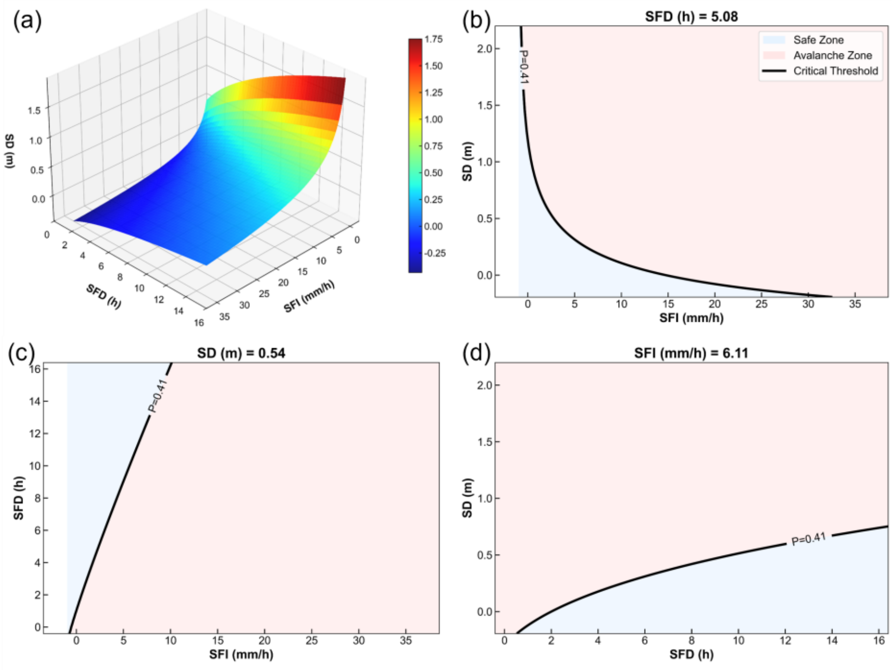

Figure 7: Three-dimensional (3D) visualization of the dry-snow avalanche SMLM and its two-dimensional (2D) projections. (a) 3D representation of the SMLM showing the joint relationship among SFI, SFD, and SD; the surface colour denotes SD. (b–d) 2D cross-sectional projections of the model-derived threshold surface, with the third variable fixed at its mean value. The black solid line represents the critical threshold boundary. The red and blue shaded regions indicate the high-probability and low-probability avalanche regimes relative to the critical threshold, respectively. The mean value of the fixed variable is indicated above each projection.

3.2.2 Wet-snow avalanches

Analogous to the dry-snow avalanche analysis, we first constructed the wet-snow avalanche MOLM:

$$\ln\left(\frac{P}{1-P}\right) = -0.08 + 2.27\ \ln(1+\mathrm{SMI}) - 0.93\ \ln(1+\mathrm{SMD})\,, \tag{11}$$

In this baseline model, the regression coefficient for SMI is positive and statistically significant (95% CI [1.70, 2.82]), and the coefficient for SMD is negative and also statistically significant (95% CI [−1.63, −0.44]). However, as with the dry-snow MOLM, this baseline model does not account for the influence of varying background snow depth on the model-derived critical boundary. To address this limitation, SD was incorporated as a predictor representing pre-event snowpack conditions to construct the integrated wet-snow SMLM, formulated as follows:

$$\ln\left(\frac{P}{1-P}\right) = -0.25 + 1.37\ln(1+\mathrm{SMI}) - 1.49\ln(1+\mathrm{SMD}) + 2.68\ln(1+\mathrm{SD})\,, \tag{12}$$

Within the wet-snow SMLM, the regression coefficient for SD remains positive and exhibits the largest magnitude ($w_3 = 2.68$; 95% CI [1.82, 3.40]). Its confidence interval lies entirely above zero, indicating that greater background snow depth is associated with a higher probability of wet-snow avalanche occurrence when SMI and SMD are held constant. The coefficient for SMI is positive and substantial ($w_1 = 1.37$; 95% CI [0.67, 2.02]), indicating a positive association between melt intensity

https://doi.org/10.5194/egusphere-2026-4540
Preprint. Discussion started: 30 July 2026

and wet-snow avalanche occurrence. Furthermore, the regression coefficient for SMD is negative ($w_2 = -1.49; 95\%\ \mathrm{CI}\ [-1.97, -1.10]$), indicating that the duration of the melting process acts as a negative modulating factor for wet-snow avalanche occurrence.

The modelling results (Fig. 8a) delineate the model-derived critical surface for wet-snow avalanches within the three-dimensional feature space of SMI, SMD, and SD, with the optimal classification probability threshold identified as 0.49. The two-dimensional cross-sectional projections further reveal that the three variables exert distinct influences on the position and shape of the critical boundary. Within the SMI–SD plane (Fig. 8b), the critical boundary exhibits a pronounced nonlinear decreasing trend. This pattern indicates that higher SMI increases avalanche-occurrence probability, allowing the system to exceed the critical probability threshold even when SD is relatively low. In the SMI–SMD plane (Fig. 8c), the critical boundary is characterised by a positive slope. According to the model-classified probability regimes, high SMI can drive the system into the high-probability avalanche regime even when SMD is relatively short. Conversely, under low-SMI conditions, the system tends to remain below the critical probability threshold even if SMD is prolonged. In the SMD–SD plane (Fig. 8d), when SMI is held constant, the critical boundary exhibits an overall nonlinear ascending trend with increasing SMD, indicating that a higher SD is required to reach the critical probability threshold as SMD increases. Overall, the wet-snow avalanche SMLM indicates that SMI and SD primarily determine the position of the critical threshold surface, whereas SMD exerts a secondary modulating effect.

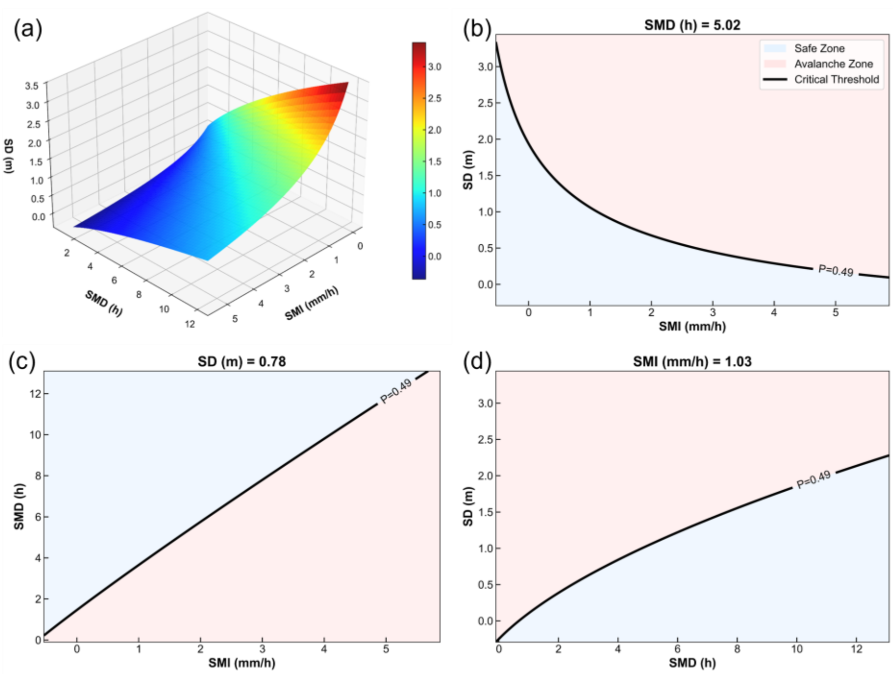

Figure 8: Three-dimensional (3D) visualization of the wet-snow avalanche SMLM and its two-dimensional (2D) projections. (a) 3D representation of the SMLM showing the joint relationship among SMI, SMD, and SD; the surface colour denotes SD. (b–d) 2D cross-sectional projections of the model-derived threshold surface, with the third variable fixed at its mean value. The black solid line represents the critical threshold boundary. The red and blue shaded regions indicate the high-probability and low-probability

https://doi.org/10.5194/egusphere-2026-4540
Preprint. Discussion started: 30 July 2026

avalanche regimes relative to the critical threshold, respectively. The mean value of the fixed variable is indicated above each projection.

3.3 Model performance

To assess the discriminative capacity of the SMLM, we compared its overall classification performance with that of the baseline MOLM using the LOOCV-derived predictions. The ROC curve analysis indicates that the SMLM consistently achieves better discrimination than the MOLM for both dry- and wet-snow avalanche scenarios (Fig. 9). Specifically, for dry-snow avalanches, the AUC increased from 0.72 for the MOLM to 0.83 for the SMLM. For wet-snow avalanches, the AUC increased from 0.85 for the MOLM to 0.94 for the SMLM. These results demonstrate that incorporating information on snowpack conditions substantially improves the discriminative performance of the SMLM.

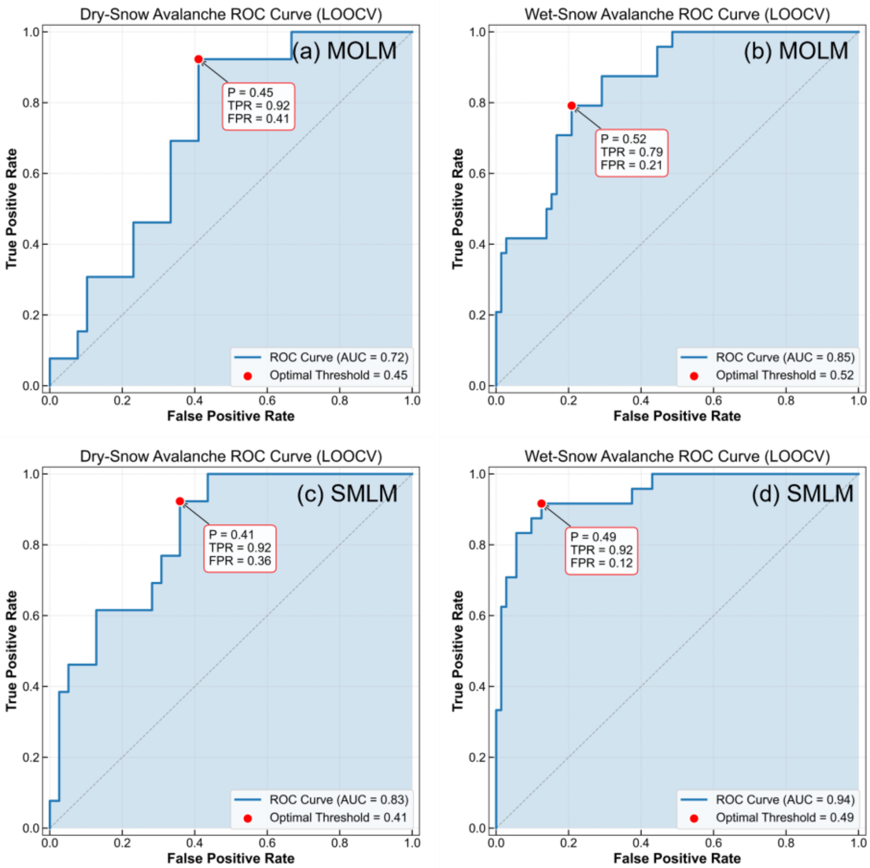

Figure 9: ROC curves and AUC comparison between the MOLM and SMLM for dry- and wet-snow avalanches under LOOCV. (a) Dry-snow avalanche MOLM; (b) wet-snow avalanche MOLM; (c) dry-snow avalanche SMLM; and (d) wet-snow avalanche SMLM.

The SMLM demonstrates a more effective trade-off between false alarms and missed events. For wet-snow avalanches, the MOLM yields an FPR of 0.21 and a Precision of 0.56. In contrast, the SMLM substantially reduces the FPR to 0.12 while increasing the Precision to 0.71. This improvement indicates a marked reduction in false alarms, accompanied by an increase

https://doi.org/10.5194/egusphere-2026-4540
Preprint. Discussion started: 30 July 2026

in TPR from 0.79 to 0.92 and a decrease in FNR from 0.21 to 0.08. For dry-snow avalanches, the FPR decreased from 0.41 to 0.36, while precision increased from 0.43 to 0.46. Overall, the SMLM improved discrimination and false-alarm control for both avalanche types, with the improvement being more pronounced for wet-snow avalanches.

Table 2. Comparison of classification performance metrics between the MOLM and SMLM.

	Wet MOLM	Dry MOLM	Wet SMLM	Dry SMLM
TPR	0.79	0.92	0.92	0.92
FPR	0.21	0.41	0.12	0.36
TNR	0.79	0.59	0.88	0.64
FNR	0.21	0.08	0.08	0.08
Precision	0.56	0.43	0.71	0.46
F1	0.66	0.59	0.80	0.62

From the perspective of operational forecasting, FNR and FPR are critical metrics because they represent missed events and false alarms, respectively. Across both avalanche scenarios, the SMLM maintained a low FNR while reducing the FPR relative to the MOLM. These results indicate that incorporating background snow depth accounts for part of the variability in pre-event snowpack conditions that is not represented by meteorological forcing alone. Compared with the baseline MOLM, the SMLM therefore provides better overall discrimination and false-alarm control, particularly for wet-snow avalanches.

4. Discussion

4.1 Physical mechanisms of avalanche triggering

Under specific topographic conditions, avalanche initiation is primarily governed by the coupled effects of meteorological forcing and snowpack conditions. The model demonstrates that SD, as a key state variable representing the pre-event snowpack conditions, exerts a strong and consistently positive influence on the occurrence probabilities of both dry- and wet-snow avalanches. This finding is consistent with previous studies suggesting that a deeper snowpack can increase overburden load and shear stress acting on potential weak layers, thereby bringing the snowpack progressively closer to a critical stress–strength threshold under additional meteorological forcing (Deems et al., 2015; Meloche et al., 2024; Schweizer et al., 2003a).

Regarding meteorological forcing conditions, the snowpack system exhibits distinct response characteristics during the initiation of dry- and wet-snow avalanches. In the wet-snow avalanche model, the positive and statistically significant coefficient for SMI indicates that rapid meltwater input is associated with an increased probability of wet-snow avalanche occurrence. Rapid snowmelt alters the snowpack stratigraphy, facilitating the percolation and subsequent accumulation of liquid water within the snow layers. This dynamic process profoundly weakens inter-granular bonding and elevates pore water pressure, thereby reducing effective stress and ultimately triggering shear failure (Conway and Raymond, 1993; Mitterer et al., 2011). By contrast, the response to SFI in the dry-snow avalanche model is more closely related to progressive mechanical loading. Snowfall increases the gravitational load of newly accumulated snow (McClung, 2020; Schweizer et al., 2003a),

https://doi.org/10.5194/egusphere-2026-4540
Preprint. Discussion started: 30 July 2026

while concurrent processes such as settlement, compaction, and stress redistribution may partly modulate the destabilizing effect of loading. Therefore, dry-snow avalanche initiation is better interpreted as a progressive reduction in slope stability under sustained snowfall loading.

Existing studies have rarely examined the role of snowfall or snowmelt duration in modulating avalanche initiation. Our modelling results indicate that both SFD for dry-snow avalanches and SMD for wet-snow avalanches exert a distinct negative effect on avalanche occurrence probability, suggesting that duration acts as a stabilizing modulator under certain forcing conditions. The physical basis of this pattern lies in the time-dependent evolution of snowpack microstructure, stress redistribution, and hydraulic properties. For dry-snow avalanches, the model shows that under low-to-moderate SFI conditions, the critical threshold increases with increasing SFD (Fig. 7c). This feature is associated with the temporal effects during the snow-loading process. When the meteorological loading rate is relatively low, a prolonged SFD provides sufficient time for microstructural adjustment within the snow layers. During this period, the new snow undergoes settlement and compaction under its own weight, while the sintering between ice crystals continuously strengthens, leading to an increase in the overall density and cohesion of the snowpack. Simultaneously, the process of viscous creep within the snow layers helps dissipate a portion of the accumulated shear stress. Consequently, slow and sustained loading may promote partial structural strengthening, requiring stronger external forcing for the snowpack to reach critical instability (Schweizer et al., 2003a). For wet-snow avalanches, the results indicate that under moderate SMI, the critical threshold also increases with increasing SMD, meaning a greater SD is required to trigger an avalanche (Fig. 8d). This behaviour is related to internal meltwater migration and wet-snow metamorphism. During the early stage of melting, liquid-water input can weaken intergranular bonds and increase local loading, thereby increasing the probability of instability. However, as melting persists, provided that abrupt strength loss or failure does not occur, preferential flow paths gradually form within the snowpack, enhancing drainage capacity and mitigating the sustained accumulation of pore water pressure on the sliding surface (Wever et al., 2016). Concurrently, prolonged wet conditions can promote snowpack settlement and densification, which may partially enhance bulk shear resistance. Therefore, with increasing SMD, the snowpack may undergo partial restabilization, and instability is more likely to occur only when the pre-event snowpack conditions is sufficiently deep, corresponding to higher background snow depth.

In summary, the triggering processes of different avalanche types reflect the complex coupling between meteorological forcing and snowpack conditions. Specifically, SD, together with SFI or SMI, governs the loading conditions and stress state within the snowpack, thereby influencing the likelihood of structural failure. In contrast, SFD and SMD modulate the critical initiation conditions by affecting the time-dependent evolution of snowpack microstructure, stress redistribution, and meltwater migration. Consequently, snowpack instability is determined not only by the intensity of external forcing but also by the combined effects of loading duration and the pre-event snowpack conditions. These findings provide a possible process-based interpretation of the model-derived shifts in critical thresholds and provide a process-based basis for developing refined regional avalanche forecasting models that jointly account for forcing intensity, forcing duration, and snowpack conditions.

4.2 Model performance and false alarm reduction

Previous studies have explored various forecasting methodologies for different avalanche types. For dry-snow avalanches, mechanistic models such as the Snowfall-triggered Avalanche Warning (SFAW) model, which represents weak-layer failure processes, have achieved a hit rate of 0.75 (Hao et al., 2022). Building on this framework, integrated approaches that couple one-dimensional snowpack simulations with meteorological forcing and apply Random Forest algorithms have further increased the dry-snow avalanche hit rate to approximately 0.79 (Mayer et al., 2023). For wet-snow avalanches, threshold based models using liquid-water indices have reported hit rates of approximately 0.80 (Bellaire et al., 2017).

Despite these advances, existing models still face important operational limitations. First, the hit rates of conventional classifiers may decrease sharply under extreme hazard conditions, reaching values as low as 0.03 in some cases (Pérez-Guillén et al., 2022). Second, models based solely on liquid-water indices or meteorological thresholds often have difficulty identifying the termination phase of wet-snow avalanche cycles, which can result in persistently high false alarm rates (Bellaire et al., 2017). It should be noted that, because of differences in training and validation datasets, temporal resolution, study regions, and evaluation protocols, the following comparisons are intended only to provide contextual evidence for the performance gains associated with the refined modelling framework, rather than to support a direct one-to-one benchmark comparison.

Based on the LOOCV results, the SMLM improved overall discrimination and false-alarm control for both avalanche types. The model achieved a hit rate of 0.92 for both dry- and wet-snow avalanches, with corresponding FPRs of 0.36 and 0.12, respectively. Two aspects of the overall modelling framework are relevant to this performance.

(1) Differentiating avalanche types improves model adaptability by accounting for their distinct triggering conditions. By developing separate logistic regression models for dry- and wet-snow avalanches, this study avoids combining events governed by different triggering processes, thereby improving type-specific discrimination performance.

(2) The improvement of the SMLM over the MOLM demonstrates the contribution of background snow depth in representing pre-event snowpack conditions. By integrating SD with meteorological forcing variables, the SMLM achieved better discrimination between avalanche and non-avalanche conditions, suggesting that antecedent snowpack state provides complementary information beyond short-term forcing alone.

4.3 Illustrative hierarchical probability framework

The aforementioned results indicate that the coupling between pre-event snowpack conditions and meteorological forcing plays an important role in avalanche occurrence, providing a methodological basis for regional probabilistic forecasting. Traditional approaches often rely on discrete meteorological thresholds, which may produce unstable classifications when conditions are close to the decision boundary. The continuous occurrence probabilities derived from the SMLM provide a means of moving beyond binary threshold-based classification and representing gradual changes in avalanche likelihood. For illustrative purposes, the modelled probabilities were divided into five equal-width categories (< 0.2, 0.2–0.4, 0.4–0.6, 0.6–0.8, and ≥ 0.8). These probability categories provide a more detailed representation of the transition from relatively low to

https://doi.org/10.5194/egusphere-2026-4540
Preprint. Discussion started: 30 July 2026

high avalanche likelihood as meteorological forcing and snowpack conditions evolve. These probability categories should be interpreted as an illustrative representation of model outputs rather than operational warning levels, which require further calibration and validation for specific applications.

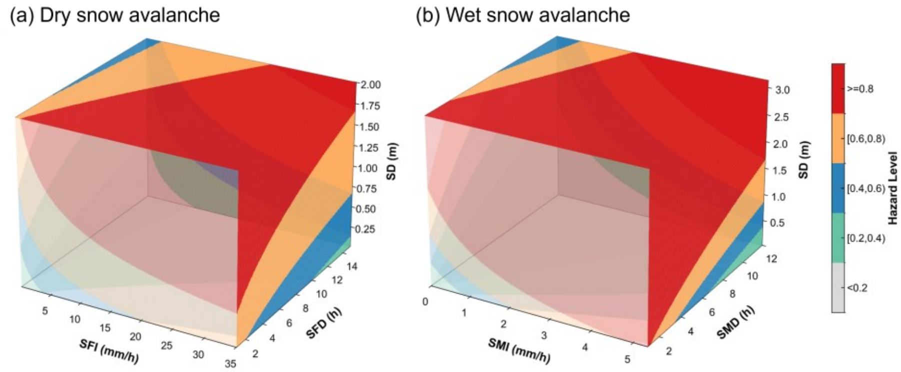

Figure 10: SMLM-derived hierarchical forecasting framework for dry- and wet-snow avalanches based on continuous occurrence probability gradients.

4.4 Limitations and future perspectives

While this study demonstrates the potential of the SMLM, several limitations remain. At the data level, although the monitoring stations capture the environmental characteristics of typical avalanche zones in southeastern Tibet, high-altitude meteorological conditions, snowpack evolution, and topographical factors exhibit substantial spatial heterogeneity. Observations from a limited number of stations may therefore be insufficient to fully characterise the regional-scale complexity of actual snowpack conditions. Consequently, the threshold relationships revealed by the model may be partly conditioned by site-specific factors when extrapolated to broader spatial domains. At the methodological level, although the LR model effectively quantifies the probabilistic relationships between loading intensity, duration, and background snow depth, it remains fundamentally an empirical-statistical model. Therefore, the threshold relationships derived in this study should be interpreted as empirical representations of multivariable coupling rather than a fully physical depiction of avalanche triggering mechanisms.

Future research should focus on integrating physical mechanisms into the modelling framework. Incorporating snowpack stability indices or mechanistic constraints within the existing statistical structure could improve the model's physical consistency and generalization capability. Furthermore, the integration of topographic factors and spatially distributed input data to extend the model toward regional-scale applications remains a critical objective for developing robust and operational avalanche forecasting systems.

https://doi.org/10.5194/egusphere-2026-4540
Preprint. Discussion started: 30 July 2026

5. Conclusions

In this study, we developed an integrated avalanche forecasting model that combines background snow depth with snowfall- or snowmelt-process variables. By utilizing variables derived from field monitoring stations and employing logistic regression to characterize conditional probabilities, this approach advances conventional meteorological-threshold models toward a state-constrained framework for identifying critical instability conditions. The findings demonstrate that SD, which represents the pre-event snowpack conditions, and the meteorological forcing intensity (SFI/SMI) are key variables associated with avalanche instability. Meanwhile, the forcing duration (SFD/SMD) appears to modulate avalanche occurrence through its influence on the time-dependent evolution of the snowpack. In terms of predictive performance, the SMLM achieved better discrimination for both avalanche types and improved false-alarm control, with the improvement being more pronounced for wet-snow avalanches. These gains were primarily associated with the incorporation of background snow depth into the forecasting framework. Compared with baseline models that excluded snowpack-condition variables, the SMLM maintained high hit rates (TPR = 0.92 for both dry- and wet-snow avalanches), increased the AUC from 0.72 to 0.83 for dry-snow avalanches and from 0.85 to 0.94 for wet-snow avalanches, and reduced the FPR from 0.41 to 0.36 and from 0.21 to 0.12, respectively. These results demonstrate the potential of the model to represent multivariable probability boundaries and support the integration of antecedent snowpack conditions into probabilistic avalanche forecasting frameworks.

Code and data availability

The processed dataset used in this study, including meteorological indicators, snowpack conditions variables, avalanche-type labels, and binary avalanche occurrence records, and the Python scripts used for the SMLM and MOLM modelling have been deposited in Zenodo at https://doi.org/10.5281/zenodo.21634873. The repository contains the input files and scripts required to reproduce the logistic regression modelling, leave-one-out cross-validation, model performance evaluation, and the key figures presented in this study. The raw high-resolution monitoring-station observations are not publicly available because of institutional confidentiality agreements and data-use restrictions. Nevertheless, the processed dataset provided in the repository preserves the key variables required for the analyses and is sufficient to reproduce the statistical modelling and evaluation results reported in this paper.

Author contributions

X.F. conducted the data processing, data analysis, figure preparation, and manuscript writing. J.H. supervised the research and contributed to manuscript review and editing. P.C. and Y.W. provided scientific guidance and contributed to manuscript revision. G.C. contributed to manuscript review. All authors read and approved the final manuscript.

Competing interests

The contact author has declared that none of the authors has any competing interests.

Acknowledgements

We thank the field teams involved in the avalanche observations and maintenance of the monitoring network.

Financial support

This work was supported by the Science and Technology Projects of the Xizang Autonomous Region, China (Grant No. XZ202601ZD0009), and the Strategic Priority Research Program of the Chinese Academy of Sciences (Grant No. XDB1390000).

References

Acharya, A., Steiner, J. F., Walizada, K. M., Ali, S., Zakir, Z. H., Caiserman, A., and Watanabe, T.: Review article: Snow and ice avalanches in high mountain asia – scientific, local and indigenous knowledge, Nat. Hazards Earth Syst. Sci., 23, 2569–2592, https://doi.org/10.5194/nhess-23-2569-2023, 2023.

Baggi, S. and Schweizer, J.: Characteristics of wet-snow avalanche activity: 20 years of observations from a high alpine valley (Dischma, Switzerland), Nat Hazards, 50, 97–108, https://doi.org/10.1007/s11069-008-9322-7, 2009.

Bellaire, S., Van Herwijnen, A., Mitterer, C., and Schweizer, J.: On forecasting wet-snow avalanche activity using simulated snow cover data, Cold Regions Science and Technology, 144, 28–38, https://doi.org/10.1016/j.coldregions.2017.09.013, 2017.

Conway, H. and Raymond, C. F.: Snow stability during rain, J. Glaciol., 39, https://doi.org/10.3189/S0022143000016531, 1993.

Deems, J. S., Gadomski, P. J., Vellone, D., Evanczyk, R., LeWinter, A. L., Birkeland, K. W., and Finnegan, D. C.: Mapping starting zone snow depth with a ground-based lidar to assist avalanche control and forecasting, Cold Reg. Sci. Technol., 120, 197–204, https://doi.org/10.1016/j.coldregions.2015.09.002, 2015.

Efron, B. and Tibshirani, R.: Bootstrap methods for standard errors, confidence intervals, and other measures of statistical accuracy, Stat. Sci., 1, 54–75, https://doi.org/10.1214/ss/1177013815, 1986.

Fawcett, T.: An introduction to ROC analysis, Pattern Recognit. Lett., 27, 861–874, https://doi.org/10.1016/j.patrec.2005.10.010, 2006.

Fu, X., Hao, J., Cui, P., Wang, Y., and Chen, G.: Dataset and Python code supporting "Forecasting different types of avalanches based on snowpack and snowfall/snowmelt conditions on the Southeastern Tibetan Plateau", Zenodo [dataset], https://doi.org/10.5281/zenodo.21634873, 2026.

Hao, J., Mind'je, R., Zhang, X., Wang, Y., Zhou, H., and Li, L.: Implementation of an early warning for snowfall-triggered avalanche to road safety in the tianshan mountains, Cold Reg. Sci. Technol., 204, 103675, https://doi.org/10.1016/j.coldregions.2022.103675, 2022.

Hastie, T., Tibshirani, R., and Friedman, J.: The elements of statistical learning: Data mining, inference, and prediction, 2nd ed., Springer, New York, https://doi.org/10.1007/978-0-387-84858-7, 2009.

Hendrick, M., Techel, F., Volpi, M., Olevski, T., Pérez-Guillén, C., van Herwijnen, A., and Schweizer, J.: Automated prediction of wet-snow avalanche activity in the swiss alps, J. Glaciol., 69, 1365–1378, https://doi.org/10.1017/jog.2023.24, 2023.

Li, C., Hao, J., Zhang, G., Wang, Y., Fang, H., Hou, W., and Cui, P.: Extreme snowfall variations in the southeastern tibetan plateau under warming climate, Atmos. Res., 311, 107690, https://doi.org/10.1016/j.atmosres.2024.107690, 2024.

Marienthal, A., Hendrikx, J., Birkeland, K. W., and Irvine, K. M.: Meteorological variables to aid forecasting deep slab avalanches on persistent weak layers, Cold Regions Science and Technology, 120, 227–236, https://doi.org/10.1016/j.coldregions.2015.08.007, 2015.

Mayer, S., Techel, F., Schweizer, J., and van Herwijnen, A.: Prediction of natural dry-snow avalanche activity using physics-based snowpack simulations, Nat. Hazards Earth Syst. Sci., 23, 3445–3465, https://doi.org/10.5194/nhess-23-3445-2023, 2023.

Mayer, S., Hendrick, M., Michel, A., Richter, B., Schweizer, J., Wernli, H., and van Herwijnen, A.: Impact of climate change on snow avalanche activity in the swiss alps, The Cryosphere, 18, 5495–5517, https://doi.org/10.5194/tc-18-5495-2024, 2024.

McClung, D. M.: Dry snow slab quasi-brittle fracture initiation and verification from field tests, J. Geophys. Res.: Earth Surf., 114, F01016, https://doi.org/10.1029/2007JF000913, 2009.

McClung, D. M.: Application of dynamic fracture mechanics to dry snow slab avalanche release, Int. J. Fract., https://doi.org/10.1007/s10704-020-00497-5, 2020.

Meloche, F., Guillet, L., Gauthier, F., Langlois, A., and Gaume, J.: Influence of slab depth spatial variability on skier-triggering probability and avalanche size, Ann. Glaciol., 65, 1–15, https://doi.org/10.1017/aog.2024.3, 2024.

Mitterer, C. and Schweizer, J.: Analysis of the snow-atmosphere energy balance during wet-snow instabilities and implications for avalanche prediction, The Cryosphere, 7, 205–216, https://doi.org/10.5194/tc-7-205-2013, 2013.

Mitterer, C., Hirashima, H., and Schweizer, J.: Wet-snow instabilities: Comparison of measured and modelled liquid water content and snow stratigraphy, Annals of Glaciology, 52, 201–208, 2011.

Monti, F., Gaume, J., Van Herwijnen, A., and Schweizer, J.: Snow instability evaluation: calculating the skier-induced stress in a multi-layered snowpack, Nat. Hazards Earth Syst. Sci., 16, 775–788, https://doi.org/10.5194/nhess-16-775-2016, 2016.

Morin, S., Horton, S., Techel, F., Bavay, M., Coléou, C., Fierz, C., Gobiet, A., Hagenmuller, P., Lafaysse, M., Mitterer, C., Monti, F., Müller, K., Pittman, M., Schirmer, M., Vionnet, V., and Schweizer, J.: Application of physical snowpack models in support of operational avalanche hazard forecasting: A status report on current implementations and prospects for the future, Cold Regions Science and Technology, 170, 102910, https://doi.org/10.1016/j.coldregions.2019.102910, 2020.

https://doi.org/10.5194/egusphere-2026-4540
Preprint. Discussion started: 30 July 2026

Pérez-Guillén, C., Techel, F., Hendrick, M., Volpi, M., van Herwijnen, A., Olevski, T., and Schweizer, J.: Data-driven automated predictions of the avalanche danger level for dry-snow conditions in switzerland, Nat. Hazards Earth Syst. Sci., 22, 2031–2056, https://doi.org/10.5194/nhess-22-2031-2022, 2022.

Schweizer, J., Jamieson, B. J., and Schneebeli, M.: Snow avalanche formation, Rev. Geophys., 41, 1016, https://doi.org/10.1029/2002RG000123, 2003a.

Schweizer, J., Kronholm, K., and Wiesinger, T.: Verification of regional snowpack stability and avalanche danger, Cold Regions Science and Technology, 37, 277–288, https://doi.org/10.1016/S0165-232X(03)00070-3, 2003b.

Wei, H., Wang, Y., Wang, S., Hao, J., Chen, G., and Fu, X.: Study on the snowfall amount triggering regional avalanches in southeastern tibet, Water, 17, 1631, https://doi.org/10.3390/w17111631, 2025.

Wen, H., Wu, X., Shu, X., Wang, D., Zhao, S., Zhou, G., and Li, X.: Spatial heterogeneity and temporal tendency of channeled snow avalanche activity retrieved from landsat images in the maritime snow climate of the parlung tsangpo catchment, southeastern tibet, Cold Regions Science and Technology, 223, 104206, https://doi.org/10.1016/j.coldregions.2024.104206, 2024.

Wever, N., Würzer, S., Fierz, C., and Lehning, M.: Simulating ice layer formation under the presence of preferential flow in layered snowpacks, The Cryosphere, 10, 2731–2744, https://doi.org/10.5194/tc-10-2731-2016, 2016.

Youden, W. J.: Index for rating diagnostic tests, Cancer, 3, 32–35, https://doi.org/10.1002/1097-0142(1950)3:1%3C32::AID-CNCR2820030106%3E3.0.CO;2-3, 1950.

Yuan, X., Yang, K., Lu, H., Wang, Y., and Ma, X.: Impacts of moisture transport through and over the yarlung tsangpo grand canyon on precipitation in the eastern tibetan plateau, Atmospheric Research, 282, 106533, https://doi.org/10.1016/j.atmosres.2022.106533, 2023.

Zuur, A. F., Ieno, E. N., and Elphick, C. S.: A protocol for data exploration to avoid common statistical problems, Methods Ecol. Evol., 1, 3–14, https://doi.org/10.1111/j.2041-210X.2009.00001.x, 2010.